# Galactosylceramide Domain Microstructure: Impact of Cholesterol and Nucleation/Growth Conditions

Craig D. Blanchette,* Wan-Chen Lin,* Timothy V. Ratto,‡ and Marjorie L. Longo†

*Biophysics Graduate Group, Division of Biological Sciences, and †Department of Chemical Engineering and Materials Science, University of California, Davis, California 95616; and ‡Biophysical and Interfacial Science Group, Chemistry and Materials Science, Lawrence Livermore National Laboratory, Livermore, California 94550

ABSTRACT Galactosylceramide (GalCer), a glycosphingolipid, is believed to exist in the extracellular leaflet of cell membranes in nanometer-sized domains or rafts. The local clustering of GalCer within rafts is thought to facilitate the initial adhesion of certain viruses, including HIV-1, and bacteria to cells through multivalent interactions between receptor proteins (gp120 for HIV-1) and GalCer. Here we use atomic force microscopy (AFM) to study the effects of cholesterol on solid-phase GalCer domain microstructure and miscibility with a fluid lipid 1,2-dilauroyl-*sn*-glycero-3-phosphocholine (DLPC) in supported lipid bilayers. Using "slow-cooled vesicle fusion" to prepare the supported lipid bilayers, we were able to overcome the nonequilibrium effects of the substrate (verified by comparison to results for giant unilamellar vesicles) and accurately quantify the dramatic effect of cholesterol on the GalCer domain surface area/perimeter ratio ($A_D/P$) and DLPC-GalCer miscibility. We compare these results to a supported lipid bilayer system in which the bilayer is rapidly cooled (nonequilibrium conditions), "quenched vesicle fusion", and find that the microstructures are remarkably similar above a cholesterol mol fraction of ~0.06. We determined that GalCer domains were contained in one leaflet distal to the mica substrate through qualitative binding experiments with *Trichosanthes kirilowii* agglutinin (TKA), a galactose-specific lectin, and AFM of Langmuir-Blodgett deposited GalCer/DLPC supported lipid bilayers. In addition, GalCer domains in bilayers containing cholesterol rearranged upon tip-sample contact. Our results further serve to clarify why discrepancies exist between different model membrane systems and between model membranes and cell membranes. In addition, these results offer new insight into the effect of cholesterol and surrounding lipid on domain microstructure and behavior. Finally, our observations may be pertinent to cell membrane structure, dynamics, and HIV infection.

## INTRODUCTION

An issue of central importance in membrane biology is the possible existence and function of microdomains, referred to as rafts, within the plane of the cellular membrane. Over the past decade there has been an emergence of evidence indicating cell membranes do not exist as a homogeneous lipid matrix, as was described in the fluid mosaic model (1), but rather certain lipid constituents (glycosphingolipids, cholesterol, and sphingomyelin) may phase separate into microdomains or rafts (2–6). Rafts are believed to serve several functions, which include signaling, sorting, and trafficking through secretory and endocytic pathways (3,7) and acting as attachment platforms for host pathogens and their toxins (8).

A glycosphingolipid of particular interest and biological relevance is galactosylceramide (GalCer). GalCer has been identified as an alternative receptor for gp120, an HIV-1 envelope glycoprotein, in a variety of CD4 negative cells including neural (9,10), colonic (11,12), and vaginal (13) epithelial cells. GalCer is the major glycosphingolipid in these cell types, which have glycosphingolipid concentrations ranging from 10–20% of total membrane lipids, but it is located exclusively in the extracellular leaflet so its effective mol fraction in that leaflet is 0.2–0.4 (14). In addition a GalCer derivative, galactosylalkylacylglyercol, expressed in sperm cells has been shown to bind to gp120 with affinities similar to GalCer (15). Infection of colonic and vaginal epithelial cells is believed to result in sexual transmission of the virus. Once infected, the epithelial cells can transmit the virus to mucosal lymphocytes or macrophages through cell-to-cell contact, resulting in autoimmune deficiency syndrome (AIDS). Because GalCer has been isolated from detergent-resistant membranes (DRMs), it is believed to exist in phase-separated domains or rafts (5,16). Despite this evidence, no work has been done to study GalCer domain microstructures in model membranes. Therefore it is of essential importance to characterize the effects of cholesterol on GalCer domain microstructures to further understand the behavior of GalCer in cellular membranes.

The primary intent of this work is to quantitatively study the effects of cholesterol on GalCer domain microstructure. Accurate quantification requires a high-resolution characterization method such as atomic force microscopy, necessitating the use of lipid bilayers supported on a flat substrate (mica). Such studies on ordered phase domains have been precluded in the past because it has been shown that under the previous conditions of formation, domain microstructures for supported lipid bilayers formed through vesicle fusion are trapped at "nanoscale" microstructures far from equilibrium (17,18). Instead, reliable, yet relatively qualitative assessments on the impact of cholesterol on domain microstructure have been obtained using giant unilamellar

*Submitted October 11, 2005, and accepted for publication March 1, 2006.*

Address reprint requests to Marjorie L. Longo, Tel.: 530-754-6348; Fax: 530-752-1031; E-mail: mllongo@ucdavis.edu.



0006-3495/06/06/4466/13 $2.00

doi: 10.1529/biophysj.105.072744

vesicles (GUVs), a ''free'' bilayer system in which ''microscale'' domains for similar compositions are formed (19–24).

One of the major factors relevant to domain size is the thermal history of the bilayer, where domain growth can be greatly affected by cooling rates. Nonequilibrium domain growth, i.e., domain growth after a rapid quench, has been examined through Monte Carlo simulations and experimentally using fluorescence spectroscopy, Fourier transform infrared spectroscopy (FTIR), and time-resolved fluorescence resonance energy transfer (FRET) (25–27). From this work it was concluded that unless a sufficient equilibration period is allowed during the phase-separation process, domain structures could exist in stable long-lived nonequilibrium morphologies. In addition by rapidly cooling a membrane into the solid-liquid phase coexistence regime, the time allowed for domain growth is insufficient for micronscale domain formation. Thus this method results in small solid phase domains that must then coalesce or undergo Ostwald ripening to form larger structures which may increase the energetic barrier in the formation of equilibrium structures. This nonequilibrium effect is presumably greater for supported lipid bilayers due to bilayer-substrate interactions that prevent domains and possibly individual lipids below their $T_m$ from diffusing. These factors directly indicate that the method of bilayer preparation and thermal history will have dramatic effects on the domain microstructures, and these effects can result in kinetically and mechanically trapped domain microstructures.

Based on these ideas we believe one of the major reasons discrepancies exist in domain microstructures between GUVs (micronscale) and supported lipid bilayers (nanoscale) may be related to the different methods applied during bilayer preparation for these two model membrane systems before analyzing domain microstructures, in addition to substrate effects. There have been two primary methods applied in studying domain microstructures for GUVs displaying phase coexistence: 1), observing domains at incremental temperatures as the GUV is cooled from the fluid to solid-fluid coexistence regime and allowed to equilibrate at a given temperature (a quasi slow-cooling method) (21,28,29), and 2), slowly cooling the GUVs over a time period of several hours (19,30,31). In contrast there have been three primary methods employed for supported lipid bilayers displaying phase coexistence formed through vesicle fusion: 1), depositing a heated SUV or large unilamellar vesicle (LUV) suspension (above the $T_m$ of the lipid mixture) onto room temperature substrate, i.e., quenched vesicle fusion (18,32–34); 2), depositing room temperature SUV or LUV suspensions onto a room temperature substrate (35,36); and 3), depositing a heated SUV or LUV suspension onto a heated substrate and then letting the sample equilibrate to room temperature (37). The publications that have reported using method 3 did not specify how fast the supported lipid bilayer was cooled or equilibrated to room temperature; but based on the findings in this study and for distearoylphosphatidylcholine (DSPC)-DLPC mixtures (38), the cooling rates were not slow enough to allow for large-scale domain growth.

Therefore, to achieve our objective of quantitatively studying the effect of cholesterol on GalCer domain microstructure, we were mindful of the thermal history of the supported lipid bilayer. We used two techniques to form supported lipid bilayer containing mixtures of GalCer, cholesterol, and 1,2-dilauroyl-*sn*-glycero-3-phosphocholine (DLPC). By slow-cooled vesicle fusion, GalCer domains were formed which we demonstrate approach equilibrium by their favorable comparison to the size and shape of domains obtained using GUVs. Once this was established, we utilized one of the great advantages of supported lipid bilayers over GUVs: AFM can be used to obtain high-resolution images. By utilizing AFM to image supported lipid bilayers, we quantify for the first time, to our knowledge, the dramatic change cholesterol imposes upon the domain surface area/perimeter ratio for solid phase domains. By comparison to previous observations, we determine that the domains remain in the solid phase with increasing cholesterol mol fraction. By quenched vesicle fusion, domains were given little time to form, allowing the impact of cholesterol on domain-formation kinetics to be examined. Furthermore, qualitative binding experiments with *Trichosanthes kirilowii* agglutinin (TKA), a galactose-specific lectin, and AFM of Langmuir-Blodgett deposited GalCer/DLPC supported lipid bilayers were used to determine the symmetry and location of GalCer domains (distal or proximal to the mica surface). Simultaneously we qualitatively characterized the onset of rearrangements induced by the AFM tip in the presence of cholesterol. These results are discussed with respect to discrepancies reported between model membrane systems of various types and compositions. We suggest a possible role of cholesterol, partitioning to the domain perimeter and modulating interfacial line tension in this system. Finally, the biological implications with respect to plasma membrane structure and HIV infection are proposed. Technically GalCer domains should be regarded as GalCer rich since DLPC and cholesterol may exist in the domains at low concentrations that do not liquidize the domains.

## MATERIALS AND METHODS

### Materials

TKA conjugated with tetramethylrhodamine isothiocynate (TRITC) was purchased from EY laboratories (San Mateo, CA). GalCer (Cerebrosides, a mixture of nonhydroxylated and hydroxylated GalCer with tail lengths varying from 16 to 24 carbons; see Matreya handbook for exact tail length compositions) was purchased from Matreya (Pleasant Gap, PA). DLPC and 1-palmitoyl-2-[6-[(7-nitro-2-1,3-benzoxadiazol-4-yl)amino]hexanoyl]-*sn*-glycero-3-phosphocholine (NBD-PC) were purchased from Avanti Lipids (Alabaster, AL). Lactose, glucose, sucrose, cholesterol, and PBS (pH 7.4, 0.01 M phosphate buffer saline, 0.138 M NaCl, 0.0027 M KCl) were all purchased from Sigma chemicals (St. Louis, MO). All materials were used without further purification. All water used in these experiments was purified in a Barnstead Nanopure System (Barnstead Thermolyne, Dubuque, IA) with a resistivity equal to 17.9 MΩ and pH 5.5.

## Vesicle preparation

Vesicles were prepared from varying lipid mixtures of DLPC/GalCer with and without the addition of cholesterol. Lipid mixtures were dried in a clean glass reaction vial under a slow stream of $N_2$. The dried lipid film was resuspended with Nanopure water to a final lipid concentration of 0.5 mg/ml for high GalCer domain area coverage and 0.1 mg/ml for low domain area coverage. The lipid suspension was incubated in a 90°C water bath for 5 min followed by a 15-s vortexing period. The lipid suspension, consisting of giant multilameller vesicles (GMVs) was transferred to a plastic tube at room temperature before further treatment. A suspension of small unilameller vesicles (SUVs) was formed by sonicating the GMV suspension with a tip sonicator (Branson sonifer, model 250, Branson Ultrasonics, Danbury, CT) at the highest power until the suspension reached clarity. The suspension of SUVs was then put into a water bath at 90°C for 30 min before further use.

## Supported lipid bilayers

Two different techniques were employed for the formation of supported lipid bilayers, both utilizing vesicle fusion. For the first technique, quenched vesicle fusion, 150 $\mu$l of the heated suspension of SUVs (90°C) was deposited onto freshly cleaved room-temperature mica glued to a small metal puck. This quenching process has been shown to result in small nanoscale lipid domains, a nonequilibrium condition (18,33). The vesicle droplet was allowed to incubate on the mica disk for 30 min and then rinsed 40 times with 80-$\mu$l aliquots of purified water to remove excess vesicles. In the second technique, slow-cooled vesicle fusion, 150 $\mu$l of the heated suspension of SUVs (90°C) was deposited onto a heated mica surface (90°C) glued to a small metal puck. The mica disk was then slowly cooled to room temperature in a temperature-controlled oven. Slow cooling in the absence of cholesterol resulted in large micronscale domains, an indicator of equilibrium domain formation. After cooling, excess vesicles were removed by rinsing 40 times with 80-$\mu$l aliquots of purified water.

## AFM imaging

Samples were imaged with a Digital Instruments NanoScope IIIa (Santa Barbara, CA) in contact mode with a J scan head. Experimental details are described elsewhere (33). A public domain software package, Imagetool (University of Texas Health Center, San Antonio, TX), which can detect and measure physical parameters of the height images produced from the Digital Instruments AFM software, was used to analyze the size, perimeter, and area fraction of the solid phase domains in our supported lipid bilayer samples. Images were modified in Adobe Photoshop 4.0 to enhance contrast before analysis.

## GUV preparation

GUVs were prepared using the electroformation method (39). Lipid mixtures containing 1 mol % of NBD-PC (partitions to the fluid phase) were combined at various mol ratios (depending on the vesicle composition needed for experimentation) and dissolved in chloroform such that the final total lipid concentration was 1 mg/ml. Using a glass syringe, 50 $\mu$L of the lipid solution was coated evenly onto two parallel platinum wires separated by 3 mm. The wires were housed in the center of an open rectangular Teflon block. The solvent was evaporated under a slow flow of nitrogen gas. The remaining solvent was removed by placing the wires under vacuum for at least 2 h. The open center of the block was sealed into a chamber by two SurfaSil (Pierce Biotechnology, Rockford, IL) coated glass coverslips using vacuum grease. The chamber was filled with a 100-mM sucrose aqueous solution that had been preheated to ~90°C, i.e., above the 80°C phase transition temperature of GalCer. The chamber was then submerged in a preheated sucrose solution and placed in an oven preheated to 90°C. A series of sine waves (3 V peak to peak) were applied across the wires at 10 Hz for 30 min, 3 Hz for 15 min, 1 Hz for 7 min, and 0.5 Hz for 7 min using a function generator (Tenma, Centerville, OH). The temperature of the solution in which the chamber was submerged was carefully monitored throughout the electroformation process to make sure it did not fall below 90°C. After the electroformation was complete the chamber was slowly cooled to room temperature (~24°C) and then allowed to equilibrate for 1 h. The vesicles were then harvested in Eppendorf vials. A total of 100 $\mu$l GUV solution was then placed in a small chamber containing 100 mM glucose solution. GUVs were imaged 30 min later when the vesicles had collected at the bottom of the chamber. This method resulted in GUVs ranging in size from 10–60 $\mu$m in diameter. The GUVs were used the same day of their preparation. Fluorescent imaging was carried out with a Nikon Eclipse 400 fluorescence microscope (Nikon, Melville NY) equipped with a fluorescence filter cube (EF-4 FITC HYQ, Nikon) that matched the excitation and emission spectrum of NBD-PC. Images were captured with a high resolution Orca digital camera (Hamamatsu Photonics, Hamamatsu, Japan).

## Protein binding experiments

After imaging the bilayers with AFM, the mica disks were dropped into a petri dish containing PBS. The petri dishes were then submerged in a large glass bowl also containing PBS. The bilayers were rapidly oscillated by hand while submerged in the PBS solution to further rinse any extra vesicles adsorbed to the supported bilayer surface. Twenty microliters of TKA-TRITC from a 0.2-mg/ml stock solution was deposited directly on top of the rinsed bilayer surface. After a 30-min equilibration period, the bilayers were gently rinsed to remove excess unbound protein. Fluorescent imaging was carried out with a Nikon Eclipse 400 fluorescence microscope equipped with a TRITC (96171 M RHQ) cube that matched the excitation and emission spectrum of the TRITC probe. Images were captured with a high resolution Orca digital camera.

# RESULTS

## Supported lipid bilayers: domains approaching equilibrium at various compositions

GUVs have often been described as equilibrium model membrane systems due to the micronscale phase separation that is observed in these model membrane systems. We speculate that the discrepancies in domain microstructures that have been reported for supported lipid bilayers and GUVs is due in part to the different methods of bilayer preparation, in particular the thermal history of the bilayer before analysis. Based on this notion we developed a technique in which the supported lipid bilayer is slowly cooled during lipid phase separation or immiscibility. We call this technique ''slow-cooled vesicle fusion''. The method is based on depositing heated vesicles (90°C) onto mica contained in a 90°C oven and then slowly cooling (2–5 h) the sample to room temperature in the oven. For 0.6 DLPC: 0.4 GalCer lipid mixtures, longer cooling times resulted in larger domains as illustrated in Fig. 1, *a–c*. At the slowest cooling rate, GalCer domains grew as large as 30 $\mu$m in diameter. When domain diameters were $>15$ $\mu$m, they adopted a leaf-like shape and the domain population exhibited a bimodal domain size distribution of larger ($>15$ $\mu$m) and smaller ($<3$ $\mu$m) size domains (Fig. 1 *c*).

To determine if this method results in domain microstructures that approach equilibrium we compared the domain microstructures for supported lipid bilayers slow cooled for 5

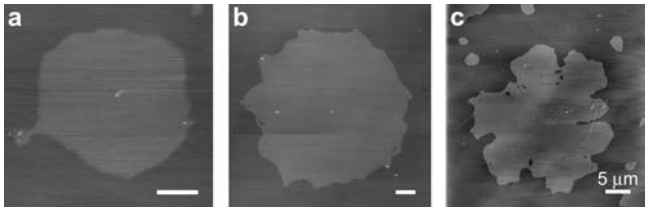


FIGURE 1 Controlling GalCer gel phase domain size through cooling rates. (*a–c*) Bilayers were formed through the slow-cooling vesicle fusion method where the bilayer was cooled from 90°C to 25°C over (*a*) a 2-h time period, (*b*) a 3-h time period, and (*c*) a 5-h time period. All bilayers were made from 0.6 DLPC: 0.4 GalCer vesicle suspensions. Scale bar 1 $\mu$m unless indicated otherwise.

h to GUVs at different lipid compositions with varying concentrations of cholesterol (Fig. 2). We chose two different DLPC compositions, one that resulted in a high GalCer domain area fraction (referred to as the H-series), and the other that resulted in a low GalCer domain area fraction (referred to as the L-series). High domain area fraction bilayers (H-series) were made from a vesicle suspension containing a 0.5-mol fraction of DLPC and a combined GalCer and cholesterol mol fraction of 0.5 (i.e., GalCer mol fraction + cholesterol mol fraction = 0.5), whereas low domain area fraction bilayers (L-series) were made from a vesicle suspension containing 0.75-mol fraction of DLPC and a combined GalCer and cholesterol mol fraction of 0.25 (i.e., GalCer mol fraction + cholesterol mol fraction = 0.25). The exact lipid compositions that were used to prepare the vesicle suspension and their corresponding letter code can be found in Table 1, and the compositional ''phase diagram'' based on the bilayer area fraction of GalCer ($D_A$) in the resulting supported lipid bilayers prepared from these vesicle suspensions is presented in Fig. 3. To calculate $D_A$, we assumed that GalCer is contained in only one leaflet in the supported bilayer (shown later) and GUVs (argued as a possibility later). Essentially L and H refer to the L-series and H-series compositions, respectively, and the number refers to the percent cholesterol in the lipid mixture. It is worth noting that the purpose of this section and Fig. 2 is only to demonstrate that slow-cooling methods result in very similar domain morphologies for supported lipid bilayers and GUVs at varying membrane compositions. A more detailed presentation of the effects of cholesterol on equilibrium GalCer domains and the compositional ''phase diagram'' (Fig. 3) is presented below.

We chose nine different lipid compositions for comparison of domain microstructures between GUVs and slow-cooled supported lipid bilayers: L-0, L-5, L-10, L-12.5, H-0, H-10, H-25, and H-30 (Fig. 2). In these experiments we used the exact same lipid compositions to form the SUV suspension (for supported lipid bilayer formation) as was used to form the GUVs. During GUV formation the electroformation chamber was kept at 90°C to ensure all lipids were in a fluid state. After vesicle formation was complete, the GUV suspension was slowly cooled (~2 h) to room temperature and then harvested after 1 h at room tempera-

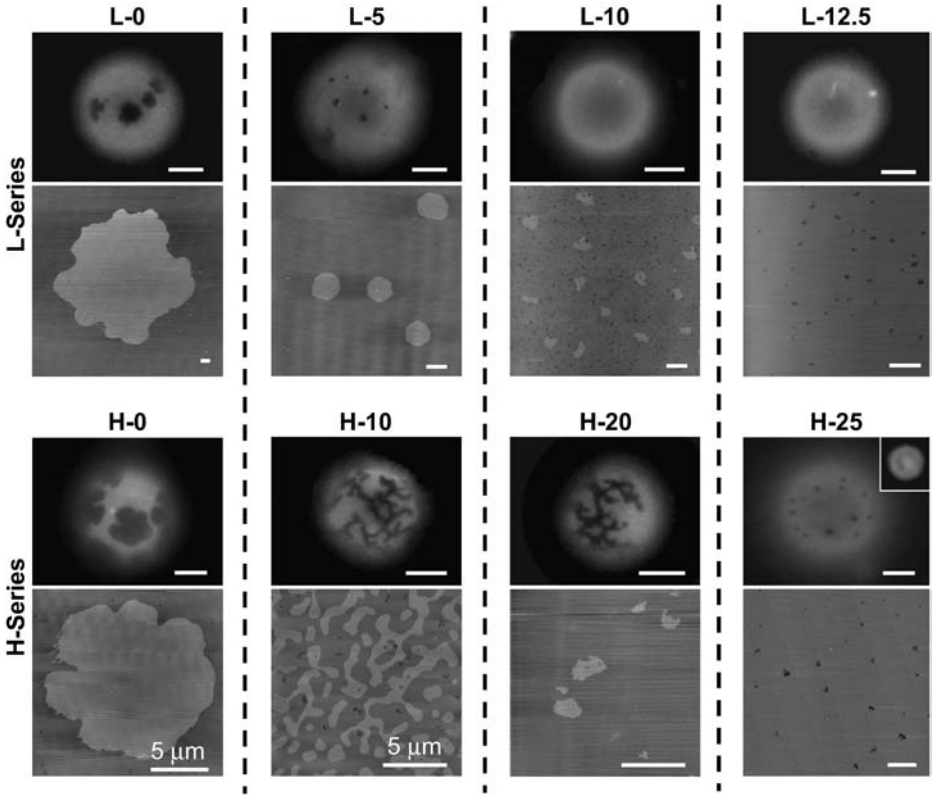


FIGURE 2 GalCer domain microstructure for slow-cooled supported lipid bilayers and GUVs, an unsupported equilibrium model membrane system. The top set of images corresponds to the L-series compositions (refer to Table 1). Domain size and shape were consistent at all compositions. The disappearance of observable domains at L-10 in the GUVs results from the lower resolution of optical fluorescence microscopy. The bottom set of images corresponds to the H-series compositions. Domain size and shape were consistent at all compositions except H-20 and H-25. At H-20 the domains in GUVs maintained the networked domain microstructures whereas the domains in slow-cooled supported bilayers adopted small irregular shaped ovals. At H-25 GalCer and DLPC became miscible in slow-cooled bilayers whereas in GUVs we observed circular domains that were at the resolution limit of optical fluorescence microscopy. At H-30 no domains were observed in GUVs, indicating lipid miscibility (*inset*). Fluorescence scale bar 10 $\mu$m. AFM scale bar 1 $\mu$m, unless indicated otherwise.

**TABLE 1 Lipid compositions and corresponding letter codes**

| Lipid composition for L - series | | | | Lipid composition for H - series | | | |
|---|---|---|---|---|---|---|---|
| Letter code | DLPC | GalCer | Cholesterol | Letter code | DLPC | GalCer | Cholesterol |
| L-0 | 0.75 | 0.25 | 0 | H-0 | 0.5 | 0.5 | 0 |
| L-3 | 0.75 | 0.22 | 0.03 | H-2 | 0.5 | 0.48 | 0.02 |
| L-4 | 0.75 | 0.21 | 0.04 | H-5 | 0.5 | 0.45 | 0.05 |
| L-5 | 0.75 | 0.2 | 0.05 | H-7.5 | 0.5 | 0.425 | 0.075 |
| L-6 | 0.75 | 0.1875 | 0.0625 | H-10 | 0.5 | 0.4 | 0.1 |
| L-7.5 | 0.75 | 0.175 | 0.075 | H-17.5 | 0.5 | 0.325 | 0.175 |
| L-10 | 0.75 | 0.15 | 0.1 | H-20 | 0.5 | 0.3 | 0.2 |
| L-12 | 0.75 | 0.13 | 0.12 | H-25 | 0.5 | 0.25 | 0.25 |
| L-12.5 | 0.75 | 0.125 | 0.125 | H-30 | 0.5 | 0.2 | 0.3 |

ture. This protocol was chosen because it was the method used by several groups that have investigated lipid phase coexistence under conditions where domain microstructures exhibited micronscale phase separation, i.e., domain microstructures approached equilibrium morphologies (19,30,31,40). GUVs were doped with 1 mol % NBD-PC, which partitions to the less-ordered phase; therefore the dark regions in Fig. 2 represent the more ordered phase. The depth of field of the objective used in the fluorescent GUV images was smaller than the size of the vesicles, so only surface morphologies were imaged, i.e., the images shown in Fig. 2 are the top or bottom of the GUV vesicles and the actual diameters of the vesicles are larger than they appear in the fluorescent images. It is worth noting that the GUVs imaged in Fig. 2 were chosen because $D_A$ was similar to $D_A$ observed in the supported lipid bilayer.

One of the differences we observed between slow-cooled supported lipid bilayers and GUVs were at compositions where the GalCer domains were several microns (L-0 and H-0). At these compositions the domains in supported lipid bilayers tended to be slightly larger. This discrepancy probably occurs because the total membrane area for a supported lipid bilayer is several orders of magnitude larger than GUVs. Therefore the maximum domain radius in GUVs is limited by the size of the GUV. To limit this discrepancy we observed the largest GUVs in the population. In addition, we never observed a bimodal domain distribution in the GUVs, which indicated that only the larger domains in slow-cooled bilayers displaying bimodal distributions approached equilibrium.

The GalCer domain microstructures for GUVs was very similar in both shape and size to the slow-cooled supported lipid bilayers at all the lipid compositions in the L-series (Fig. 2, top AFM images). At the L-10 composition, domain diameters for slow-cooled supported lipid bilayers were maximally ~200 nm, so the lack of domains in GUVs may be due to the limiting optical resolution of our fluorescent microscope.

At the H-10 composition, domains in GUVs displayed a networked morphology also observed for slow-cooled supported lipid bilayers. But at the H-20 composition, the domains in GUVs maintained the networked domain microstructures whereas the domains in slow-cooled supported lipid bilayers adopted small irregular oval shaped domains. At H-25, the GUVs displayed very small pixelated domains, which were at the resolution limit of our optical fluorescence microscope. At this cholesterol mol fraction the domains more closely resembled the microstructures we observed at H-20 in slow-cooled supported lipid bilayers. At H-30 the GUVs appeared homogeneous, indicating GalCer-DLPC miscibility. We examined H-20, H-25, and H-30 using Texas Red 1,2-dihexadecanoylphosphatidylethanolamine (TR-DHPE) as a probe for the less condensed regions, and the results were identical. The discrepancy between GUVs and supported

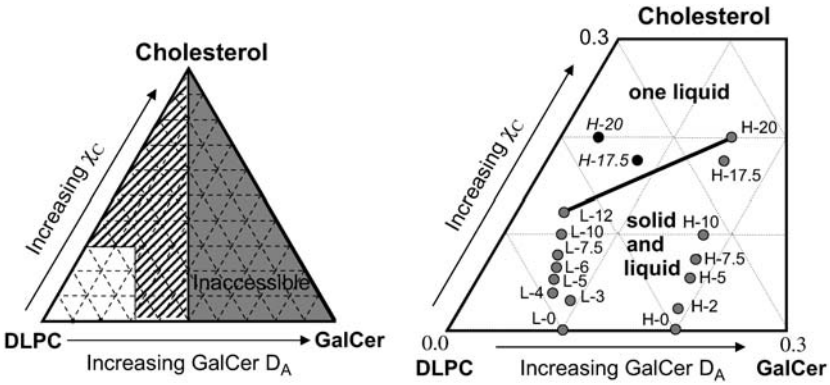


FIGURE 3 Compositional phase diagram for the ternary DLPC: GalCer: cholesterol mixtures based on the bilayer area fraction of the GalCer domains ($D_A$). The left side displays the entire phase space. Since the GalCer domains are in one leaflet, the highest $D_A$ accessible is 0.5. The right side displays the region of the phase diagram we examined. Each dot in this phase diagram is labeled with a letter code indicating the composition of the vesicle suspension used to make the supported lipid bilayer (refer to Table 1 for the exact composition for each letter code). For the H-series compositions we observed a dramatic drop in GalCer domain area fraction for H-17.5 and H-20 compositions (*black circles*), which we believe is due to partial GalCer solubility in the fluid phase. Thus we have estimated the actual compositions based on the trends seen in the rest of the H-series for H-17.5 and H-20 (*gray circles*). The black line between L-12 and H-20 indicates the phase boundary between solid-liquid coexistence and one liquid.

lipid bilayers at H-20 through H-30 may be a result of a slightly different DLPC/GalCer/cholesterol ratio in the GUVs compared to the supported lipid bilayer. Indeed, lipid compositions that exist in lipid mixtures used to make GUVs and supported lipid bilayers are not an exact reflection of the compositions of the GUVs or supported lipid bilayers. Despite this discrepancy, the qualitative correlation between domain size and shape for most of the lipid compositions indicate that slow cooling in supported lipid bilayers results in domain microstructures that approach equilibrium.

### Effect of cholesterol on equilibrium GalCer domain microstructure and domain growth rates

Having established that the method of slow-cooling vesicle fusion results in domain microstructures that are approaching equilibrium, we conducted these slow-cooling experiments at a larger range of cholesterol mol fractions to better estimate the effect of cholesterol on the equilibrium microstructure of GalCer domains and DLPC-GalCer miscibility. All supported lipid bilayers were cooled from 90°C–24°C over a 5-h time period. Table 1 summarizes all the different compositions we used. We have observed that the lipid composition used to prepare the vesicle suspensions do not accurately reflect the lipid composition of the resulting supported lipid bilayer. As a result we have also included a compositional ''phase diagram'' in Fig. 3, which is based on the measured domain area fraction of GalCer. The bottom axis of the ''phase diagram'' in Fig. 3 is presented as the bilayer area fraction ($D_A$) of GalCer as analyzed from the AFM images, which at lower cholesterol mol fractions, $\chi_C$ ($<0.10$), we believe much more accurately represent the actual composition of the bilayer. This is evident by comparing the GalCer mol fractions in the vesicle suspension with $D_A$ in the resulting bilayer at the various lipid compositions (Table 1 versus Fig. 3); the GalCer mol fraction is often more than double $D_A$. The top set of AFM images in Fig. 4 corresponds to the L-series compositions given in Table 1 and Fig. 3. The maximum domain diameter obtained for the L-0 composition was $\sim$15 $\mu$m. The domains displayed a bimodal distribution of $\sim$15 $\mu$m and $\sim$2 $\mu$m. As the cholesterol mol fraction, $\chi_C$, was increased (L-0 to L-12.5—left to right), we observed a cholesterol-dependent decrease in domain diameter. We observed a bimodal domain size distribution at L-3 but it was shifted to smaller domain diameters of larger $>5$ $\mu$m and smaller $<1$ $\mu$m. At increasing $\chi_C$ values, only one dominant size was observed. For compositions ranging from L-10–L-12.5, GalCer domains reached a maximum diameter of $\sim$200 nm. To quantify the effects of cholesterol on domain microstructure, domain surface area/perimeter ratios ($A_D/P$) were analyzed at varying $\chi_C$ for the L-series and H-series. For compositions where we observed a bimodal domain size distribution, we showed by comparison to GUVs that only the larger domain sizes approach equilibrium domain microstructures. Therefore only the $A_D/P$ for the larger domains were analyzed. Analysis of the domain microstructure for the L-series compositions revealed a dramatic drop in $A_D/P$ between 0.04 ($A_D/P = 1.8$ $\mu$m) and 0.075 ($A_D/P = 0.11$ $\mu$m) $\chi_C$ (Fig. 4—*graph*). There was no significant change in $A_D/P$ upon addition of cholesterol at $\chi_C \geq 0.075$. At the L-12.5 composition, phase separation was no longer observed indicating that GalCer and DLPC became miscible at this cholesterol concentration.

The bottom set of images in Fig. 4 corresponds to the H-series compositions given in Table 1 and Fig. 3. With no cholesterol present (H-0), domains reached a maximum diameter of $\sim$25 $\mu$m. The domains displayed a bimodal distribution of $\sim$25 $\mu$m and $\sim$3 $\mu$m. At the H-2 composition we again observed a bimodal domain size distribution where the larger domain diameters were $\sim$18 $\mu$m and the smaller domain diameters were $\sim$2 $\mu$m. Between H-5 and H-10 compositions, the domains adopted a branching network structure (see H-7.5). Above 0.10 $\chi_C$ GalCer domains were nanoscale irregular-shaped ovals as opposed to networked (Fig. 4). In addition at these higher cholesterol mol fractions ($\chi_C > 0.1$, H-17.5 and H-20), the $D_A$ dramatically dropped ($\sim$0.1) relative to the GalCer mol fraction that was added to the initial vesicle solution used to form the bilayer. We speculate that at these higher cholesterol mol fractions a large portion of GalCer has become soluble within the DLPC-rich fluid phase, thus $D_A$ is no longer an accurate measure of the bilayer composition. Therefore to establish a more accurate compositional ''phase diagram'' at these cholesterol mol fractions, we assumed the lipid compositions followed the same trends for the rest of the H series (Fig. 3, *gray circles* H-17.5 and H-20). Analysis of the domain microstructure for the H-series compositions revealed a dramatic drop in $A_D/P$ from 2.96 $\mu$m to 0.12 $\mu$m between $\chi_C = 0.02$ and 0.05 (where the domain microstructure goes from micronscale circular domains to a branching network configuration) (Fig. 4, *graph*). Upon further addition of cholesterol, there was no significant change in $A_D/P$. At the H-25 composition, domains were no longer observed, indicating complete GalCer-DLPC miscibility. Therefore, the cholesterol mol fraction at which GalCer and DLPC became miscible appears to increase as the concentration of GalCer in the bilayer increases.

To determine cholesterol's effect on the time to reach equilibrium, we used a second technique to prepare supported lipid bilayers: quenched vesicle fusion. Quenched vesicle fusion involves depositing a suspension of heated vesicles (90°C) onto room temperature mica (33). This technique is based on the notion of rapidly cooling a two-component bilayer past the solid-liquid phase transition temperature ($T_m$) of one of the components (GalCer in this case), thus limiting the time for domain growth and immobilizing domains of this component on the nanoscale. By using the two methods of slow cooling and quenching, we can determine cholesterol's effects on the time to reach equilibrium domain microstructures . In the absence of cholesterol, bilayers formed through quenched vesicle fusion exhibit nanoscale circular GalCer

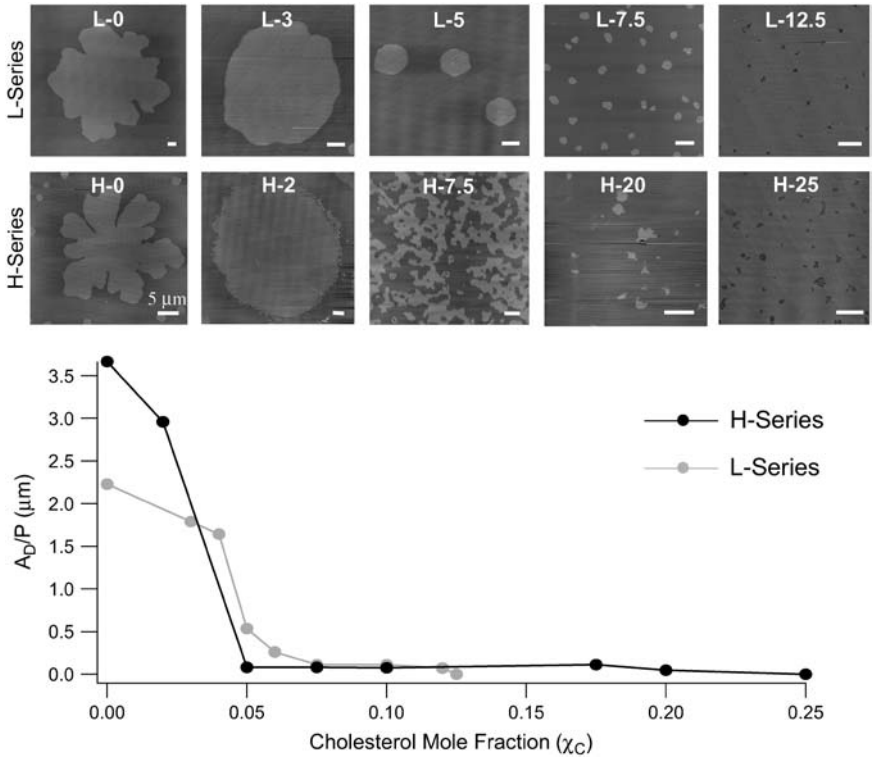


FIGURE 4 Effect of bilayer area fraction of GalCer ($D_A$) and cholesterol mol fraction ($\chi_C$) on domain microstructure and domain area/perimeter ratio ($A_D/P$) for slow-cooled bilayers. The top set of AFM images examines the effects of cholesterol for the L-series compositions. $\chi_C$ increases from left to right. At L-12.5, GalCer become miscible with DLPC and domain formation was no longer observed. The bottom set of AFM images examines the effects of cholesterol for the H-series compositions. At H-25, GalCer becomes miscible with DLPC and domain formation was no longer observed. The graph is the $A_D/P$ for L-series compositions (*gray line*) and H-series compositions (*black line*). For the H-series compositions there is a dramatic drop in $A_D/P$ (2.96–0.081 $\mu$m) between 0.02 and 0.05 $\chi_C$. For the L-series compositions there is a similar drop in $A_D/P$ (1.8–0.11) between 0.03 and 0.75 $\chi_C$. Scale bar 1 $\mu$m unless indicated otherwise.

domains, as opposed to the equilibrium micronscale leaf-like domain microstructures we observed for slow-cooled bilayers (Fig. 5). These results indicate that the time to reach equilibrium domain microstructures was very long when cholesterol was not present in the bilayer. These quenching experiments were repeated at H-5 and L-7.5 lipid compositions. These two compositions were chosen because at higher cholesterol concentrations we no longer observed any changes in $A_D/P$ when slow-cooled vesicle fusion was used to prepare the supported bilayers. For H-5 and L-7.5 both quenched vesicle fusion and slow cooling resulted in identical domain microstructures (Fig. 5). At L-7.5, GalCer domains were nanoscale circular discs (~300 nm in diameter), and at H-5 GalCer domains were highly branched and networked (Fig. 5). These results indicate that the addition of cholesterol can modulate the time to reach equilibrium domain microstructures.

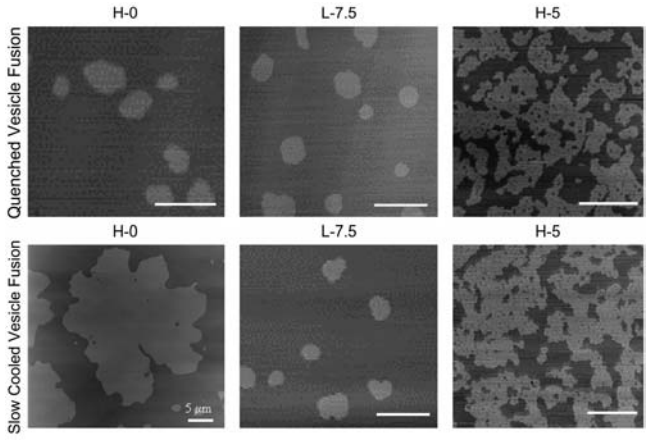


FIGURE 5 Comparing domain microstructure for bilayers formed through quenched vesicle fusion and slow-cooling vesicle fusion at H-0, L-7.5, and H-5 lipid compositions.

## GalCer domains: symmetry state, leaflet heterogeneity, and domain rearrangement

A total of 250 GalCer domain heights were analyzed from 12 different bilayers formed through both slow cooling and quenched vesicle fusion, and a histogram of domain height was constructed (Fig. 6 *a*). The mean domain height was 0.9 nm. The predominant GalCer acyl chain length for the mixture used in this study was 18 carbons. The domain height for symmetric DSPC (18 carbon acyl chain) domains in DSPC: DLPC bilayers has been previously reported to be ~1.8 nm (33,34). Based on these observations the 0.9 nm domain height measured in our system suggests the bilayers were asymmetric and the GalCer domains were not symmetrically superimposed across both leaflets. Langmuir-Blodgett deposition was utilized to determine if the observed 0.9 nm height difference was consistent with the notion of asymmetry between the bilayer leaflets. During Langmuir-Blodgett deposition of phase separated lipids, the phases of

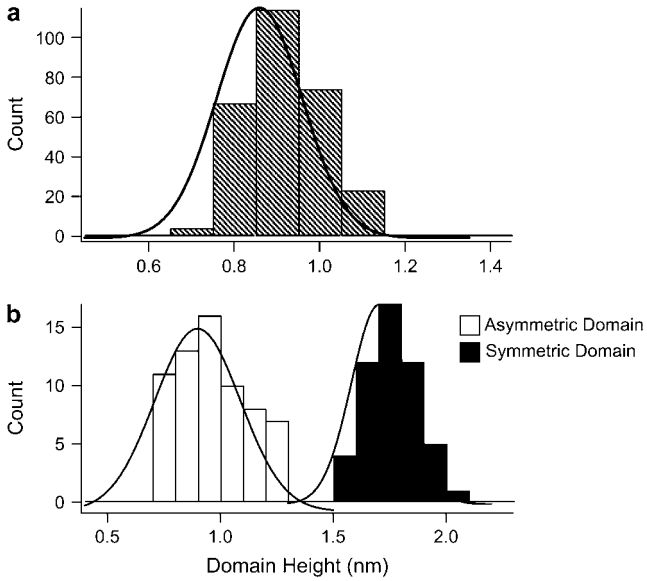


FIGURE 6 Data demonstrating that GalCer domains formed through vesicle fusion display transbilayer asymmetry. (*a*) Domain height histogram for 250 domains for bilayers formed through quenched and slow-cooling vesicle fusion. The mean domain height under these conditions was 0.9 nm. (*b*) 1:1 mol ratio of GalCer/DLPC were transferred to each monolayer through Langmuir-Blodgett deposition. This technique resulted in asymmetric, symmetric, and partially symmetric GalCer domains. Domain heights were analyzed for 120 symmetric (*dark bars*) and asymmetric (*white bars*) domains. The asymmetric and symmetric height distributions were centered at 0.95 nm and 1.75 nm, respectively.

each monolayer do not perfectly superimpose, resulting in symmetric, asymmetric, and partial symmetric solid phase regions (17,41). We used a 1:1 lipid ratio of GalCer/DLPC in both leaflets, and domain heights were measured and analyzed for 120 domains. There were two peaks in the height distribution centered at 0.95 nm (asymmetric domains) and 1.75 nm (symmetric domains) (Fig. 6 *b*). These results indicate that the domains formed through vesicle fusion are asymmetric.

For GUVs, GalCer domains exhibited the same fluorescence intensity as the background, indicating that the fluorescent probe was excluded from both leaflets in the region of the GalCer domains. This results suggest that either GalCer domains in GUVs are superimposed in both leaflets (symmetric domains) or that ordered domains in one leaflet (asymmetric domains) are inducing order in the opposing leaflet.

Since protein binding is limited to the monolayer exposed to the solvent, we have developed qualitative binding experiments to elucidate which monolayer asymmetric GalCer domains preferentially partition. For these experiments we chose to use TKA, a galactose-specific lectin. The results of these binding experiments are displayed in Fig. 7. Bilayers with and without the addition of cholesterol formed through quenched vesicle fusion (L-0, L-5) bind TKA at all cholesterol mol fractions (Fig. 7). Since GalCer domain size formed through this technique was on the nanoscale, no correlation could be made between binding pattern and domain microstructure, but these results do indicate some of the domains must partition to the distal monolayer. Domains formed through slow cooling were on the micronscale, which is well within the resolution of optical microscopy. Upon addition of TKA to L-0 and L-3 slow-cooled bilayers, we observe a TKA binding pattern that strongly reflects the GalCer microstructure imaged by AFM (Fig. 7). To determine if the TKA-GalCer binding was specific, we conducted control experiments in 100-$\mu$M lactose solution (TKA has been shown to have a higher binding affinity for lactose) and binding was blocked (data not shown). By adding a fluorescent probe to the fluid phase we have observed that the increased TKA binding around the domain perimeter (as indicated by the bright fluorescent ring) at the L-3 composition was actually outside the domain (data not shown). We believe this may have occurred because GalCer exists in low concentrations just outside the domain perimeter, resulting in increased TKA-GalCer binding affinity due to increased ligand spacing. Despite this, the strong correlation between the fluorescent binding pattern and domain size and density

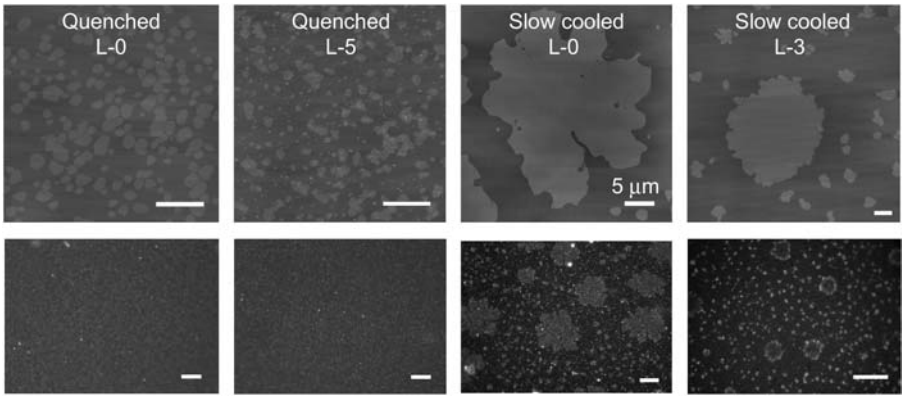


FIGURE 7 TKA binding to supported lipid bilayer containing GalCer domains of varying size and cholesterol content. The top set of images is AFM images of the supported lipid bilayers before addition of TKA-TRITC. The bottom set of images is fluorescence microscopy images of the bilayer after addition of TKA-TRITC. Upon addition of TKA-TRITC to bilayers formed through quenched vesicle fusion we see a speckled fluorescent binding pattern indicating some of the GalCer domains must be partitioned to the distal leaflet. Due to the small size of GalCer domains formed through this technique, no comparison can be made between domain microstructure and binding pattern. When TKA was deposited onto bilayers formed through slow cooling, a fluorescent binding pattern that strongly corresponds to GalCer domain microstructure was observed. Scale bar for AFM and fluorescent images are 1 $\mu$m and 10 $\mu$m unless indicated otherwise.

indicates most asymmetric domains exist in the distal monolayer.

In the absence of cholesterol, GalCer domains did not change size or shape 3 h after formation regardless of the number of scans and the scanning force. In contrast, for domains that adopt branching network microstructures (i.e., H-5, H-7.5, and H-10) the domains rearranged after AFM-tip sample contact (Fig. 8). Over a series of consecutive scans, some GalCer domains became gradually wider and more elongated, whereas others gradually disappeared as they were merged (bit by bit) to the larger domains. This behavior appears to be dependent on tip-sample contact and was examined by scanning the same area ~10 consecutive times and monitoring changes in domain microstructure. The change in domain microstructure for ~10 consecutive scans was much more dramatic than the changes that occurred over the same time period for regions that were scanned only twice (data not shown), indicating that the tip was physically remodeling the domains during the scanning process. This occurred at even the lowest scanning forces; however, the changes in domain microstructure were not as dramatic. In addition once the domains became wider and trapped fluid pools were squeezed out, domain rearrangement was no longer observed. It is worth noting that the supported lipid bilayer images shown in the previous section that displayed networked morphologies were the first scan of that region; therefore, they did not include domain rearrangement.

## DISCUSSION

### Previous discrepancy in domain size and domain growth rates between GUVs and supported lipid bilayers

Our results demonstrate that being mindful of thermal history is essential in domain formation in supported lipid bilayers. For example, by using a slow-cooling method, we could form supported lipid bilayers with GalCer domain microstructures strikingly similar to those found in GUVs. Indeed, our results suggest that the inconsistencies in domain microstructures that have been reported between GUVs and supported lipid bilayers (formed through vesicle fusion) are in part due to the thermal history of the bilayer when each model membrane system has been studied. Therefore it is of great importance that any future work conducted with supported lipid bilayers or GUVs begin to address issues of cooling rate and thermal history before drawing any significant conclusions about phase behavior and domain formation. As we demonstrate here, attention to these issues will help eliminate inconsistencies with regard to domain microstructures that have been observed between different model membrane systems. In addition the slow-cooling methods presented in this work may expand the role supported lipid bilayers play in studying lipid phase behavior and the effects of sterols on domain microstructures and domain perimeter line tension.

Less clear is the role of the substrate in domain growth in supported lipid bilayers relative to GUVs. Since there is only a thin water layer (~1 nm) insulating the bilayer from the substrate in supported lipid bilayers, it is quite plausible that the substrate alters the rate and/or mechanism of domain growth. One obvious difference is the bimodal domain distribution in supported lipid bilayers at low cholesterol concentrations. It is possible that in supported lipid bilayers the substrate induces more nucleation sites relative to GUVs and only a percentage of them grow. Very little has been done to study domain characteristics after quenching in GUVs such that comparisons could be made to supported lipid bilayers. The role of the substrate is a subject that should be addressed further because of its relevance in terms of the function and existence of membrane rafts. It has been postulated that the cell may play an active role in regulating and inducing nucleation sites within the plasma membrane by delivering small molecules that act as nucleation centers (7); therefore, understanding the relationship between domain growth and external thermodynamic parameters may provide further insight into the organization of cellular membranes.

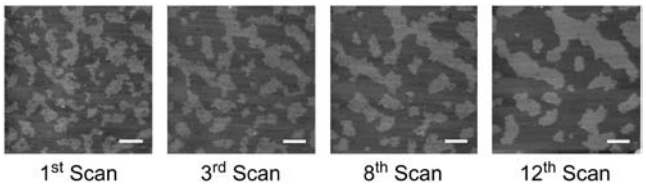


FIGURE 8 GalCer domains containing cholesterol rearrange upon AFM tip-sample contact. The bilayer in the above images was formed from the H-7.5 vesicle composition and was scanned 12 times consecutively. Through the course of 12 consecutive scans the domains began to clump into larger domains and became thicker and more extended. This process appears to depend on tip-sample contact. After scanning one region for several hours and moving the tip to a different region, the domain microstructure had not changed relative to the first scan of the original region imaged. Therefore the tip is physically moving and clumping these domains together. Scale bar 1 $\mu$m.

### Effects of cholesterol on domain perimeter line tension and the time for domain growth

One of the most striking results of this work is the dramatic drop in $A_D/P$ between 0.03–0.05 and 0.0375–0.075 cholesterol mol fractions for the H- and L-series, respectively (Fig. 4 *graph*). For the DOPC: dipalmitoylphosphatidylcholine (DPPC): sphingomyelin system, Veatch and Keller also showed images of a change in morphology for solid domains at low cholesterol content (23). However, this phenomenon was not discussed or quantified. Quantification would have been difficult because the cooling rate was not particularly slow and because GUVs were used, preventing high resolution imaging to accurately determine $A_D/P$ values. We believe this dramatic change in $A_D/P$ reflects the partitioning properties of cholesterol for the domain interface. Line ten-

sion is primarily dictated by the size of the hydrophobic mismatch between the two phases. Through computer simulations and theoretical analysis, it has been extensively documented that lipids both stretch and deform at the perimeter interface to compensate for the hydrophobic mismatch and prevent hydrophobic exposure (25,27,42,43). Therefore, bilayers exhibiting phase separation can be divided into three physically different environments: the domain phase, the fluid phase, and the interface between the two phases. Thus cholesterol will exhibit different partitioning for these three regions. As discussed in more detail below, we believe cholesterol is primarily located in the fluid phase; therefore, this dramatic drop in line tension cannot be explained through a change in macroscopic mechanical properties that may be propagated to the interface because at these low cholesterol mol fractions very few mechanical changes occur in the fluid phase (44). Thus, we believe that the fluid phase may act as a reservoir of cholesterol for partitioning to the domain interface and that an equilibrium exists between cholesterol located at the interface and fluid phase. We believe that once the concentration in the fluid phase passes a threshold, a cooperative transition occurs in which cholesterol's affinity for DLPC at the solid domain interface is greatly increased. The increase in cholesterol at the domain interface should result in a stiffening of the perimeter DLPC chains and in increasing their length, (45) thus decreasing the hydrophobic mismatch and line tension. This would explain why we observe a sudden drop in $A_D/P$ within a small cholesterol mol fraction range. Based on this argument, this process may occur at lower cholesterol mol fractions for H-series compositions because the fluid phase area is smaller; thus the effective concentration of cholesterol in the fluid phase is higher. It is worth noting that the percent loss of cholesterol from the fluid phase to the perimeter interface at $\chi_C$ where we believe cholesterol has saturated the interface is only 0.4% for L-series compositions and 1.2% for H-series compositions; thus very little cholesterol would be required for this process to occur and would have minimal effects on the composition of the fluid region. This argument is further supported by the fact that there appears to be a change in the compositional properties at the perimeter interface since TKA binding is directed to this region when cholesterol is present in the bilayer.

By comparing domain microstructure between quenched vesicle fusion and slow cooling, we observed an identical domain configuration at the L-7.5 composition and the H-5 composition (Fig. 5). The equilibrium size of these domains also happens to be small (submicron) or narrow (submicron) and networked. Their size is, in fact, on the scale of GalCer domains formed by quenched vesicle fusion indicating that due to their small equilibrium size, they form in about the timescale of the quenched vesicle fusion process. Therefore, the reduction in line tension by cholesterol confers upon the domains, the property of small equilibrium size and related short time to reach the equilibrium size.

## GalCer domain phase is solid, $S_o$, effect of fluid component on phase coexistence

Based upon their microstructure, the domains we have observed in both GUVs and supported lipid bilayers remain in the solid, $S_o$, phase at increasing $\chi_C$ as opposed to undergoing a phase transition into a liquid state brought about by increasing liquid-ordered, $L_o$, phase content in the domains. This conclusion is reached by comparing the microstructure to those observed at similar compositions in ternary mixtures of DOPC: DPPC: cholesterol (23), egg phosphatidylcholine: brain sphingomyelin: cholesterol (23), and DLPC: DPPC: cholesterol (19,30). Based on the behavior of ordered phase domains in these mixtures in GUVs, Veatch and Keller (23) concluded that below $\chi_C = 0.1$ and 0.2, DPPC-rich or sphingomyelin-rich domains exist in the solid phase, and the domain microstructure at these lower cholesterol mol fractions strongly resembled the networked microstructures we have observed in the H-series compositions. In addition, domain microstructure in DLPC: DPPC: cholesterol ternary mixtures exhibited networked morphologies up to $\chi_C = 0.16$ (19). Using electron spin resonance (ESR) Chiang et al. demonstrated that the DPPC-rich domains in this ternary mixture exist in the solid phase up to $\chi_C = 0.16$ (46).

We believe the lack of domains above a $\chi_C \sim 0.1$ to $\sim 0.2$ for L- and H-series compositions represents a miscibility transition. In other words, as $\chi_C$ is raised, our system goes from liquid-solid coexistence to one liquid phase with no intervening liquid-liquid regime (Fig. 3). This is consistent with recent results in ternary systems where it was found by Veatch and Keller that the presence of saturated chains in the surrounding fluid lipids severely decreased the temperature of the liquid to liquid-liquid transition at fixed compositions in comparison to a system in which the domains were surrounded with fluid lipids containing all unsaturated chains (24). In fact, the liquid-liquid coexistence regime was eliminated all together for a system containing POPC: DPPC: cholesterol (24). Similarly, Feigenson and Buboltz found that the DLPC: DPPC: cholesterol GUVs transitioned from liquid-solid coexistence to what appears to be one liquid phase at $\chi_C \sim 0.16$ (19). Above $\chi_C \sim 0.16$, the GUVs appeared completely homogeneous (no domains). Using FRET analysis these authors were able to demonstrate the existence of nanoscopic lipid domains for $\chi_C$ between 0.16 and 0.25 (19). Chiang et al. demonstrated that within this cholesterol mol fraction (0.16–0.25) the bilayer most likely exists in a coexistence of two liquid phase, one of the phases comprising nanoscopic domains in the $L_o$ phase (46). Therefore, it is plausible that within the apparent miscibility regime we observe, there exists nanometerscale $L_o$ GalCer-rich domains which we were unable to visualize in GUVs due to the resolution of optical fluorescence microscopy or in supported lipid bilayers due to a lack of phase height differences. This would explain why it appears that more cholesterol is needed to induce the miscibility transition as

the concentration of GalCer increases, i.e., at the apparent miscibility transition cholesterol is now more strongly associated with GalCer than with DLPC.

The lack of a liquid-liquid regime for our system and several others seems to be tied to the preferential partitioning of cholesterol with each lipid species. Lund-Katz et al. have demonstrated that the rate of cholesterol exchange between SUVs is approximately an order of magnitude faster when the donor vesicle contains unsaturated phosphocholines (PCs) (egg PC or DOPC) relative to donor vesicles containing saturated PCs (dimyristoylphosphatidylcholine or DPPC) (47). These results have also been extensively documented in several other laboratories (for review see Phillips et al. (48)). Since the kinetics of desorbing cholesterol from a bilayer is related to the strength of the phospholipid-cholesterol interaction, these results indicate that cholesterol has stronger interactions with saturated PCs relative to unsaturated PCs. In addition it has been shown using molecular condensation and cholesterol oxidation for GalCer (same mixture of GalCer as was used in this study) monolayers at the air-water interface that there were very weak associations between cholesterol and GalCer (49). Thus not only does cholesterol prefer fluid phase lipids containing a saturated acyl chain but cholesterol also appears to weakly interact with GalCer containing a mix of different acyl chain lengths and hydroxylation. We are currently investigating the role of the fluid phase component in regulating the distribution of cholesterol between the GalCer-rich phase and the fluid phase by employing fluid phase lipids that contain double bonds in either both acyl chains or in one, i.e., will unsaturated double bonds in the fluid lipid component result in liquid-liquid coexistence?

## Transbilayer asymmetry of GalCer domains

We have observed that GalCer domains in supported lipid bilayers formed through vesicle fusion always display an asymmetric distribution, with the domains partitioned exclusively to the distal leaflet. Several other model membrane systems including both GUVs and supported lipid bilayers have reported only symmetric solid phases in binary mixtures with fluid phase lipids (18,20–22,37). Using $^{13}C$ NMR it was shown that at low GalCer concentrations (1–2 mol %) 70% of GalCer was localized to the inner leaflet in SUVs (50). More recently Malewicz demonstrated this same effect at a higher GalCer concentration (5%) where 74.6% of GalCer was localized to the inner leaflet (51). One plausible explanation for the observed asymmetric GalCer domain distributions for bilayers formed through vesicle fusion may be related to the distribution of GalCer within the SUVs before supported lipid bilayer formation. Bilayer formation through vesicle fusion is believed to occur through four steps, initial vesicle absorption, fusion of absorbed vesicle to form larger vesicles (if the initial vesicle is not large enough for rupture), vesicle rupture forming bilayer discs on the surface, and finally merging of bilayer discs to form a uniform two-dimensional supported lipid bilayer (52–55). Therefore if GalCer is enriched in the inner leaflet of the SUV, it will be located primarily in the distal leaflet of the supported lipid bilayer. In GUVs we observed ordered GalCer domains that appeared dark in fluorescence, indicating that probe was excluded from both leaflets at those locations. These results suggest that GalCer domains were symmetric and superimposed in both leaflets, but it is plausible that this is not the case and GalCer domains in one leaflet are inducing an ordered phase in the adjacent leaflet possibly due to partial acyl chain interdigitation. If this is the case, then the lipid probe would have a significantly reduced partition coefficient for the induced ordered phase and the GUV would appear to display symmetric domain distributions. In fact, Merkel et al. have previously demonstrated this for asymmetric planar bilayers formed through Langmuir-Blodgett deposition. In this work solid domain formation in one leaflet induced order in the adjacent fluid phase leaflet, resulting in the exclusion of the fluid phase fluorescent probe (56).

## Domain immobility and the effect of cholesterol on domain rearrangement

Upon addition of cholesterol we observed that the AFM tip was capable of moving and rearranging the domains, whereas imaging in contact mode and domain rearrangement was dependent on the number of scans and scanning force (Fig. 8). We believe this effect primarily results from a loss of structural cohesiveness of the domains due to the lowered line tension and presence of fluid phase pools trapped within the domain structures. As mentioned previously we believe cholesterol is reducing domain perimeter line tension. This effect results in the formation of small fluid pools being trapped within the networked domains (Figs. 4 and 8). We believe this weakens the structural cohesive properties of the domain, which allow the AFM tip to drag small pieces of the domains across the bilayer until it clumps into adjacent domains (Fig. 7). These conclusions are supported by the observation that once the domains have become wider and the fluid pools are squeezed out, domain rearrangement is no longer observed. Thus it appears that the domains have reestablished a cohesive structure once the domains no longer contain fluid pools.

## Biological implications

There has long existed a discrepancy in domain size between model membranes, particularly GUVs, and cellular membrane rafts. This discrepancy has often been attributed to the increased complexity and dynamics of cellular membranes in comparison to model membranes. Cellular membranes are highly dynamic with both cholesterol and lipids continuously recycled at the membrane interface. Due to the constant changing membrane environment it has been hypothesized that rafts may never reach an equilibrium size, as they do for

GUVs, and thus do not display micronscale phase separation. From the work presented here we can begin to understand some of these inconsistencies. As we have shown, the observed discrepancy may be due in part to the presence of cholesterol within cellular membranes. The ability of cholesterol to suppress line tension at domain edges both decreases equilibrium domain radius to the nanoscopic regime and rapidly accelerates the time to reach equilibrium domain microstructures. Despite the highly dynamic processes associated with cellular membranes the formation of nanoscale domains may occur rapidly relative to changes in the membrane environment. The GalCer/cholesterol mol ratio in colonic intestinal cells has been reported to be ~1:1 (14). Based on the results for both L- and H-series compositions, this mol fraction is right at the point of lipid miscibility (Fig. 2). Therefore slight changes in local cholesterol and sphingolipid concentration may result in the disappearance or appearance of 100-nm scale domains, but these changes may be readily accommodated as a result of the increased rate of domain formation (or disappearance) in the presence of cholesterol. Therefore the local dynamic behavior in cellular membranes can greatly affect both the existence and function of cellular rafts. In addition it is beginning to appear that the fluid phase lipid component can have dramatic effects on the phase of ordered lipid domains, where the use of a fluid phase lipid containing a saturated acyl chain results in solid-liquid phase coexistence as opposed to liquid-liquid phase coexistence. This aspect has been largely ignored in the past work with model membranes but may play a significant role in dictating the type of phase separation that occurs in cellular membranes rafts, i.e., solid-liquid versus liquid-liquid phase coexistence. Therefore it is essential for future work in model membranes to focus on all lipid constituents to further understand both the existence and phase of cellular membrane rafts.

M.L.L. acknowledges funding by the Nanoscale Interdisciplinary Research Teams Program of the National Science Foundation (under award Nos. CHE 0210807 and award No. BES 0506602), the Center for Polymeric Interfaces and Macromolecular Assemblies (grant NSF DMR 0213618), the Materials Research Institute at Lawrence Livermore National Laboratory (MI-03-117), and a generous endowment from Joe and Essie Smith. C.D.B. acknowledges funding from the National Institutes of Health Biotechnology Training Grant of the University of California, Davis. This work was performed under the auspices of the U.S. Dept. of Energy by the University of California/Lawrence Livermore National Laboratory under contract No. W-7405-Eng-48.

## REFERENCES

1. Singer, S. J., and G. L. Nicolson. 1972. The fluid mosaic model of the structure of cell membranes. *Science*. 175:720–731.
2. Brown, D. A., and E. London. 1997. Structure of detergent-resistant membrane domains: does phase separation occur in biological membranes? *Biochem. Biophys. Res. Commun.* 240:1–7.
3. Simons, K., and E. Ikonen. 1997. Functional rafts in cell membranes. *Nature*. 387:569–572.
4. Hwang, J., L. A. Gheber, L. Margolis, and M. Edidin. 1998. Domains in cell plasma membranes investigated by near-field scanning optical microscopy. *Biophys. J.* 74:2184–2190.
5. Thompson, T. E., and T. W. Tillack. 1985. Organization of glycosphingolipids in bilayers and plasma membranes of mammalian cells. *Annu. Rev. Biophys. Biophys. Chem.* 14:361–386.
6. Brown, D. A., and E. London. 1998. Structure and origin of ordered lipid domains in biological membranes. *J. Membr. Biol.* 164: 103–114.
7. Brown, D. A., and E. London. 1998. Functions of lipid rafts in biological membranes. *Annu. Rev. Cell Dev. Biol.* 14:111–136.
8. Fantini, J., M. Maresca, D. Hammache, N. Yahi, and O. Delezay. 2000. Glycosphingolipid (GSL) microdomains as attachment platforms for host pathogens and their toxins on intestinal epithelial cells: activation of signal transduction pathways and perturbations of intestinal absorption and secretion. *Glycoconj. J.* 17:173–179.
9. Bhat, S., S. L. Spitalnik, F. Gonzalez-Scarano, and D. H. Silberberg. 1991. Galactosyl ceramide or a derivative is an essential component of the neural receptor for human immunodeficiency virus type 1 envelope glycoprotein gp120. *Proc. Natl. Acad. Sci. USA*. 88:7131–7134.
10. Harouse, J. M., S. Bhat, S. L. Spitalnik, M. Laughlin, K. Stefano, D. H. Silberberg, and F. Gonzalezscarano. 1991. Inhibition of entry of HIV-1 in neural cell-lines by antibodies against galactosyl ceramide. *Science*. 253:320–323.
11. Fantini, J., D. G. Cook, N. Nathanson, S. L. Spitalnik, and F. Gonzalez-Scarano. 1993. Infection of colonic epithelial cell lines by type 1 human immunodeficiency virus is associated with cell surface expression of galactosylceramide, a potential alternative gp120 receptor. *Proc. Natl. Acad. Sci. USA*. 90:2700–2704.
12. Yahi, N., J. M. Sabatier, P. Nickel, K. Mabrouk, F. Gonzalez-Scarano, and J. Fantini. 1994. Suramin inhibits binding of the V3 region of HIV-1 envelope glycoprotein gp120 to galactosylceramide, the receptor for HIV-1 gp120 on human colon epithelial cells. *J. Biol. Chem.* 269: 24349–24353.
13. Clapham, P. R., A. McKnight, S. Talbot, and D. Wilkinson. 1996. HIV entry into cells by CD4-independent mechanisms. *Perspect. Drug Discov. Des.* 5:83–92.
14. Simons, K., and G. Vanmeer. 1988. Lipid sorting in epithelial-cells. *Biochemistry*. 27:6197–6202.
15. Gadella, B. M., D. Hammache, G. Pieroni, B. Colenbrander, L. M. van Golde, and J. Fantini. 1998. Glycolipids as potential binding sites for HIV: topology in the sperm plasma membrane in relation to the regulation of membrane fusion. *J. Reprod. Immunol.* 41:233–253.
16. Brown, D. A., and J. K. Rose. 1992. Sorting of GPI-anchored proteins to glycolipid-enriched membrane subdomains during transport to the apical cell-surface. *Cell*. 68:533–544.
17. Stottrup, B. L., S. L. Veatch, and S. L. Keller. 2004. Nonequilibrium behavior in supported lipid membranes containing cholesterol. *Biophys. J.* 86:2942–2950.
18. Giocondi, M. C., V. Vie, E. Lesniewska, P. E. Milhiet, M. Zinke-Allmang, and C. Le Grimellec. 2001. Phase topology and growth of single domains in lipid bilayers. *Langmuir*. 17:1653–1659.
19. Feigenson, G. W., and J. T. Buboltz. 2001. Ternary phase diagram of dipalmitoyl-PC/dilauroyl-PC/cholesterol: nanoscopic domain formation driven by cholesterol. *Biophys. J.* 80:2775–2788.
20. Veatch, S. L., and S. L. Keller. 2003. Separation of liquid phases in giant vesicles of ternary mixtures of phospholipids and cholesterol. *Biophys. J.* 85:3074–3083.
21. Bagatolli, L. A., and E. Gratton. 2000. A correlation between lipid domain shape and binary phospholipid mixture composition in free standing bilayers: a two-photon fluorescence microscopy study. *Biophys. J.* 79:434–447.
22. Bagatolli, L. A., and E. Gratton. 2000. Two photon fluorescence microscopy of coexisting lipid domains in giant unilamellar vesicles of binary phospholipid mixtures. *Biophys. J.* 78:290–305.
23. Veatch, S. L., and S. L. Keller. 2002. Organization in lipid membranes containing cholesterol. *Phys. Rev. Lett.* 89:268101.
24. Veatch, S. L., and S. L. Keller. 2005. Miscibility phase diagrams of giant vesicles containing sphingomyelin. *Phys. Rev. Lett.* 94:148101.

25. Jorgensen, K., A. Klinger, and R. L. Biltonen. 2000. Nonequilibrium lipid domain growth in the gel-fluid two-phase region of a DC16PC-DC22PC lipid mixture investigated by Monte Carlo computer simulation, FT-IR, and fluorescence spectroscopy. *J. Phys. Chem. B*. 104: 11763–11773.

26. de Almeida, R. F. M., L. M. S. Loura, A. Fedorov, and M. Prieto. 2002. Nonequilibrium phenomena in the phase separation of a two-component lipid bilayer. *Biophys. J*. 82:823–834.

27. Jorgensen, K., and O. G. Mouritsen. 1995. phase-separation dynamics and lateral organization of 2-component lipid-membranes. *Biophys. J*. 69:942–954.

28. Shoemaker, S. D., and T. K. Vanderlick. 2003. Material studies of lipid vesicles in the L-alpha and L-alpha-gel coexistence regimes. *Biophys. J*. 84:998–1009.

29. Nag, K., J. S. Pao, R. R. Harbottle, F. Possmayer, N. O. Petersen, and L. A. Bagatolli. 2002. Segregation of saturated chain lipids in pulmonary surfactant films and bilayers. *Biophys. J*. 82:2041–2051.

30. Korlach, J., P. Schwille, W. W. Webb, and G. W. Feigenson. 1999. Characterization of lipid bilayer phases by confocal microscopy and fluorescence correlation spectroscopy. *Proc. Natl. Acad. Sci. USA*. 96: 8461–8466.

31. Arnulphi, C., S. A. Sanchez, M. A. Tricerri, E. Gratton, and A. Jonas. 2005. Interaction of human apolipoprotein A-I with model membranes exhibiting lipid domains. *Biophys. J*. 89:285–295.

32. Yuan, C. B., and L. J. Johnston. 2001. Atomic force microscopy studies of ganglioside GM1 domains in phosphatidylcholine and phosphatidylcholine/cholesterol bilayers. *Biophys. J*. 81:1059–1069.

33. Ratto, T. V., and M. L. Longo. 2002. Obstructed diffusion in phase-separated supported lipid bilayers: a combined atomic force microscopy and fluorescence recovery after photobleaching approach. *Biophys. J*. 83:3380–3392.

34. Lin, W-C., C. D. Blanchette, T. V. Ratto, and M. L. Longo. 2006. Lipid asymmetry in DLPC/DSPC-supported lipid bilayers: a combined AFM and fluorescence microscopy study. *Biophys. J*. 90:228–237.

35. Tokumasu, F., A. J. Jin, G. W. Feigenson, and J. A. Dvorak. 2003. Nanoscopic lipid domain dynamics revealed by atomic force microscopy. *Biophys. J*. 84:2609–2618.

36. Tokumasu, F., J. Hwang, and J. A. Dvorak. 2004. Heterogeneous molecular distribution in supported multicomponent lipid bilayers. *Langmuir*. 20:614–618.

37. Milhiet, P. E., M. C. Giocondi, and C. Le Grimellec. 2002. Cholesterol is not crucial for the existence of microdomains in kidney brush-border membrane models. *J. Biol. Chem*. 277:875–878.

38. Blanchette, C. D., T. V. Ratto, and M. L. Longo. 2006. Measuring receptor-ligand interactions at model membrane surfaces. *In* Cellular Engineering. K. MR, editor. Academic Press (Elsevier), North Holland, Amsterdam, The Netherlands. 195–211.

39. Angelova, M. I., S. I. Soleau, P. Meleard, J. F. Faucon, and P. Bothorel. 1992. Preparation of giant vesicles by external AC fields. *Prog. Colloid Polym. Sci*. 89:127–131.

40. Korlach, J., T. Baumgart, W. W. Webb, and G. W. Feigenson. 2005. Detection of motional heterogeneities in lipid bilayer membranes by dual probe fluorescence correlation spectroscopy. *Biochim. Biophys. Acta*. 1668:158–163.

41. Hollars, C. W., and R. C. Dunn. 1998. Submicron structure in L-alpha-dipalmitoylphosphatidylcholine monolayers and bilayers probed with confocal, atomic force, and near-field microscopy. *Biophys. J*. 75: 342–353.

42. Akimov, S. A., P. I. Kuzmin, J. Zimmerberg, F. S. Cohen, and Y. A. Chizmadzhev. 2004. An elastic theory for line tension at a boundary separating two lipid monolayer regions of different thickness. *J. Electroanal. Chem*. 564:13–18.

43. Kuzmin, P. I., S. A. Akimov, Y. A. Chizmadzhev, J. Zimmerberg, and F. S. Cohen. 2005. Line tension and interaction energies of membrane rafts calculated from lipid splay and tilt. *Biophys. J*. 88:1120–1133.

44. Needham, D., and R. S. Nunn. 1990. Elastic-deformation and failure of lipid bilayer-membranes containing cholesterol. *Biophys. J*. 58:997–1009.

45. Nezil, F. A., and M. Bloom. 1992. Combined influence of cholesterol and synthetic amphiphillic peptides upon bilayer thickness in model membranes. *Biophys. J*. 61:1176–1183.

46. Chiang, Y. W., Y. Shimoyama, G. W. Feigenson, and J. H. Freed. 2004. Dynamic molecular structure of DPPC-DLPC-cholesterol ternary lipid system by spin-label electron spin resonance. *Biophys. J*. 87: 2483–2496.

47. Lundkatz, S., H. M. Laboda, L. R. Mclean, and M. C. Phillips. 1988. Influence of molecular packing and phospholipid type on rates of cholesterol exchange. *Biochemistry*. 27:3416–3423.

48. Phillips, M. C., W. J. Johnson, and G. H. Rothblat. 1987. Mechanisms and consequences of cellular cholesterol exchange and transfer. *Biochim. Biophys. Acta*. 906:223–276.

49. Slotte, J. P., A. L. Ostman, E. R. Kumar, and R. Bittman. 1993. Cholesterol interacts with lactosyl and maltosyl cerebrosides but not with glucosyl or galactosyl cerebrosides in mixed monolayers. *Biochemistry*. 32:7886–7892.

50. Mattjus, P., B. Malewicz, J. T. Valiyaveettil, W. J. Baumann, R. Bittman, and R. E. Brown. 2002. Sphingomyelin modulates the transbilayer distribution of galactosylceramide in phospholipid membranes. *J. Biol. Chem*. 277:19476–19481.

51. Malewicz, B., J. T. Valiyaveettil, K. Jacob, H. S. Byun, P. Mattjus, W. J. Baumann, R. Bittman, and R. E. Brown. 2005. The 3-hydroxy group and 4,5-*trans* double bond of sphingomyelin are essential for modulation of galactosylceramide transmembrane asymmetry. *Biophys. J*. 88: 2670–2680.

52. Johnson, J. M., T. Ha, S. Chu, and S. G. Boxer. 2002. Early steps of supported bilayer formation probed by single vesicle fluorescence assays. *Biophys. J*. 83:3371–3379.

53. Keller, C. A., K. Glasmastar, V. P. Zhdanov, and B. Kasemo. 2000. Formation of supported membranes from vesicles. *Phys. Rev. Lett*. 84: 5443–5446.

54. Keller, C. A., and B. Kasemo. 1998. Surface specific kinetics of lipid vesicle adsorption measured with a quartz crystal microbalance. *Biophys. J*. 75:1397–1402.

55. Reviakine, I., and A. Brisson. 2000. Formation of supported phospholipid bilayers from unilamellar vesicles investigated by atomic force microscopy. *Langmuir*. 16:1806–1815.

56. Merkel, R., E. Sackmann, and E. Evans. 1989. Molecular friction and epitactic coupling between monolayers in supported bilayers. *J. Phys. [E]*. 50:1535–1555.